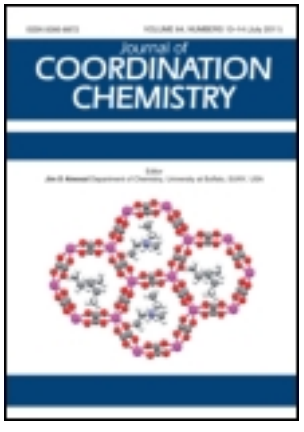

Journal of Coordination Chemistry
Publication details, including instructions for authors and subscription information:
http://www.tandfonline.com/loi/gcoo20

Complexation of the N,N′,O-donor ligand N-trans-(2′-hydroxycyclohexyl)-2-aminomethylpyridine

Vanny Tiwow [a], Geoffrey A. Lawrance [b], Marcel Maeder [b] & Paul Jensen [c]

[a] Chemistry Section, Faculty of Education, Tadulako University, Palu 94416, Indonesia

[b] Discipline of Chemistry, the University of Newcastle, Callaghan 2308, Australia

[c] School of Chemistry, University of Sydney, NSW 2006, Australia

Published online: 21 Oct 2011.

To cite this article: Vanny Tiwow, Geoffrey A. Lawrance, Marcel Maeder & Paul Jensen (2011) Complexation of the N,N′,O-donor ligand N-trans-(2′-hydroxycyclohexyl)-2-aminomethylpyridine, Journal of Coordination Chemistry, 64:20, 3637-3651, DOI: 10.1080/00958972.2011.628019

To link to this article: http://dx.doi.org/10.1080/00958972.2011.628019

Journal of Coordination Chemistry
Vol. 64, No. 20, 20 October 2011, 3637–3651

Complexation of the *N,N′,O*-donor ligand *N-trans*-(2′-hydroxycyclohexyl)-2-aminomethylpyridine

VANNY TIWOW†, GEOFFREY A. LAWRANCE*‡, MARCEL MAEDER‡ and PAUL JENSEN§

†Chemistry Section, Faculty of Education, Tadulako University, Palu 94416, Indonesia
‡Discipline of Chemistry, the University of Newcastle, Callaghan 2308, Australia
§School of Chemistry, University of Sydney, NSW 2006, Australia

(*Received 22 June 2011; in final form 2 September 2011*)

The potentially tridentate *N,N′,O*-donor *N-trans*-(2′-hydroxycyclohexyl)-2-aminomethylpyridine (**1**) forms ML_2 complexes with M(II) = Cu, Ni, and Zn. X-ray crystal structures of the isostructural Ni(II) and Zn(II) complexes confirm *bis*-tridentate coordination in significantly distorted octahedral geometries as the *all-cis facial* isomer. Structural comparisons with the previously reported *all-trans facial* Cu(II) and *cis,cis,trans*(N_{py}) *facial* Co(III) complexes are presented. Protonation constants for **1** and stability constants with Cu(II), Ni(II), and Zn(II) are reported, with both ML and ML_2 species defined. The trend for ML (log K_1 values for Cu, Ni, and Zn of 8.3, 6.9, and 5.3, respectively) is conventional. Protonation and stability constants with Cu(II) for *N,N*-bis(2-pyridylmethyl)amine (**2**) were also defined. The log K_1 value measured for **2** of 7.4 is very similar to that found for **1** of 8.3, despite the marked difference in the third donor group; it appears that the third donor of the tridentate ligand generally binds only poorly to Jahn–Teller elongated Cu(II) in solution.

Keywords: Tridentate *N,N′,O*-donor ligand; Substituted aminomethylpyridine; Metal(II) complexation; Formation constants; X-ray crystal structures

1. Introduction

The synthesis of β-amino alcohol ligands *via* ring opening of epoxides is a convenient synthetic approach [1–5], exemplified by reaction of alkane-1,2-diamines with cyclohexene oxide [5–7]. Synthesis and characterization of a new amino alcohol derived from ring opening of cyclohexene oxide with 2-aminomethylpyridine have been described [8]. *N-trans*-(2′-hydroxycyclohexyl)-2-aminomethylpyridine (**1**) is a potentially tridentate dissymmetric chiral ligand that may prove interesting due to three different potential donors: an aromatic nitrogen, an aliphatic secondary amine, and a hydroxyl. With the unsymmetrical **1** several diastereomers are possible on complexation. For octahedral coordination of two ligands as tridentate chelates, there exist six possible arrangements of the pair of ligands around an octahedral metal

*Corresponding author. Email: geoffrey.lawrance@newcastle.edu.au

ISSN 0095-8972 print/ISSN 1029-0389 online
http://dx.doi.org/10.1080/00958972.2011.628019

(figure 1), apart from any isomers associated with orientations of amine protons and optical isomers.

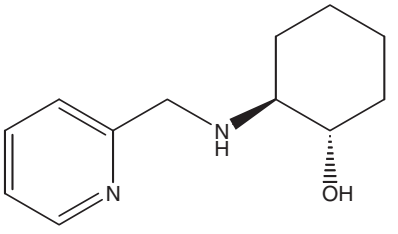

1

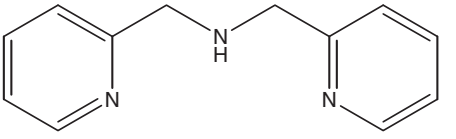

2

The focus in this work is on determination of stability constants of metal complexes of **1**, with some complexes of **1** characterized by X-ray crystal structures. Further, stability constants were determined for Cu(II) complexation of *N,N*-bis(2-pyridylmethyl)amine (**2**), which has one aliphatic and two aromatic nitrogen atoms able to coordinate to metal; it is a versatile tridentate ligand whose complexes with a range of transition metals have been reported [9–16].

2. Experimental

2.1. *Syntheses*

2.1.1. N-(2′-hydroxycyclohexyl)-2-aminomethylpyridine (1). To a solution of 20.35 g (0.188 mol) of 2-aminomethylpyridine dissolved in freshly dried EtOH (500 mL) was added 1.5 equivalents (20.2 g, 0.28 mol) of cyclohexene oxide, dropwise, with stirring. After the addition, a reflux condenser and a drying tube were fitted and the mixture was refluxed with stirring for 6 days. The solvent was then removed on a rotary evaporator and the flask was dried on a vacuum pump for a few hours, yielding a brown solid. Upon repeated recrystallization from ethyl acetate, a white crystalline product was obtained. Yield 32.9 g, 79%. Anal. Calcd for $C_{12}H_{18}N_2O$ (%): C, 69.8; H, 7.9; N, 13.5. Found (%): C, 69.4; H, 8.3; N, 13.5. Melting Point: 83.5–84°C. NMR: $\delta_H(CDCl_3)$ 0.94–2.1 (10H, m), 2.2 (1H, m), 3.2 (1H, m), 3.8 (2H, AB quartet), 7.0 (1H, t), 7.1 (1H, d), 7.5 (1H, t), 8.4 (1H, d); $\delta_C(CDCl_3)$ 24.1, 24.9, 30.8, 33.3, 51.6, 63.4, 73.6, 121.8, 122.0, 136.4, 148.8, 160.1 ppm.

2.1.2. Bis([N-(2′-hydroxycyclohexyl)-2-aminomethylpyridine)copper(II) perchlorate trihydrate, $[Cu(1)_2](ClO_4)_2 \cdot 3H_2O$. A solution of 0.27 g (1.2 mmol) of **1** was dissolved in a minimum of EtOH and added, with stirring, to a solution of 0.212 g (0.6 mmol) of copper(II) perchlorate dissolved in a small volume of EtOH. The resultant blue solution was diluted to 1.5 L with water and sorbed onto a SP-Sephadex C-25 cation exchange column ($30 \times 3\,cm^2$). Elution (0.2 mol L^{-1} $NaClO_4$) yielded a single bright blue band that was collected, concentrated and refrigerated, yielding bright blue crystals that were collected, washed in turn with small amounts of ice-cold water, ethanol, and ether, and

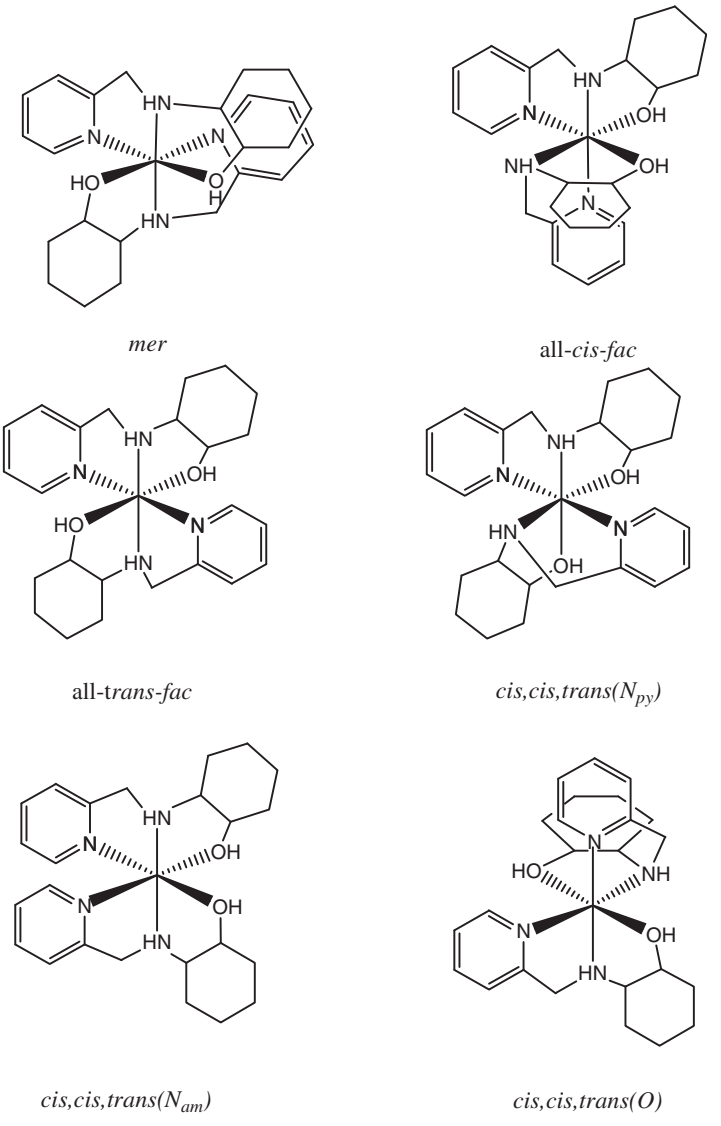

Figure 1. Geometric isomers of $[M(\mathbf{1})_2]^{n+}$ when all six donors are coordinated.

air-dried. Yield 0.37 g, 84%. Anal. Calcd for $C_{24}H_{42}N_4O_{13}CuCl_2$ (%): C, 39.55; H, 5.7; N, 7.7. Found (%): C, 39.5; H, 5.2; N, 7.7. UV-Vis (water): λ_{max} 607 nm (ϵ_{max} 46 $dm^3\,mol^{-1}\,cm^{-1}$). IR (KBr disc): 3367, 3099, 1607 (NH); 2939, 2856, 1443 (CH); 1382, 1302 (OH); 1090, 620 (ClO_4) cm^{-1}.

2.1.3. Bis(N-(2′-hydroxycyclohexyl)-2-aminomethylpyridine)nickel(II) perchlorate hemihydrate, $[Ni(1)_2](ClO_4)_2 \cdot ½H_2O$. A solution of 0.22 g (1.2 mmol) of **1** dissolved in a minimum of EtOH was added, with stirring, to a solution of 0.1 g (0.5 mmol) of

nickel(II) chloride dissolved in a small volume of EtOH. The resultant purple solution was stirred briefly, diluted to 1.5 L with water and sorbed onto a SP-Sephadex C-25 cation exchange column ($30 \times 3\,cm^2$). Elution ($0.2\,mol\,L^{-1}NaClO_4$) yielded a single bright purple band. Rotary evaporation of this purple solution to a small volume yielded, on cooling, a purple powder. This was collected, washed with a small amount of ice-cold water, then ethanol and ether, and air-dried. Yield 0.32 g, 92%. Anal. Calcd for $C_{24}H_{37}N_4O_{10.5}NiCl_2$ (%): C, 43.1; H, 5.4; N, 8.4. Found (%): C, 43.2; H, 5.4; N, 8.7. UV-Vis (water): λ_{max} 860 nm (ϵ_{max} $12\,dm^3\,mol^{-1}\,cm^{-1}$), 553 ($\epsilon$ 16). IR (KBr disc): 3420, 3168, 1622 (NH); 2939, 2856, 1443 (CH); 1374, 1340 (OH); 1104, 618 (ClO_4) cm^{-1}. A sample was recrystallized from aqueous solution by slow evaporation, with single crystals isolated as the monohydrate.

2.1.4. Bis(N-(2′-hydroxycyclohexyl)-2-aminomethylpyridine)zinc(II) perchlorate hydrate, $[Zn(1)_2](ClO_4)_2 \cdot H_2O$. A solution of 0.31 g (1.352 mmol) of **1** dissolved in a minimum of EtOH was added, with stirring, to a solution of 0.18 g (0.715 mmol) of zinc(II) perchlorate dissolved in $0.2\,mol\,L^{-1}$ $NaClO_4$. A white precipitate resulted upon addition. The mixture was stirred at room temperature for 1 h and the white solid was recovered by filtration, washed in turn with ice-cold water, ethanol, and diethyl ether, and dried. Recrystallization from water yielded X-ray quality colorless crystals, which were collected and air dried. Yield 0.39 g, 80%. Anal. Calcd for $C_{24}H_{38}N_4O_{11}ZnCl_2$ (%): C, 41.5; H, 5.5; N, 8.05. Found (%): C, 41.1; H, 5.4; N, 7.9. IR (KBr disc): 3280, 3328, 1612 (NH); 2882, 2862, 1436 (CH); 1364, 130140 (OH); 1105, 620 (ClO_4) cm^{-1}.

2.1.5. Bis((pyridine-2-yl)methyl)amine (2). This known compound was prepared by a new microwave irradiation method. A mixture of 2-pyridinecarboxaldehyde (5 mmol) and 2-aminomethylpyridine (5 mmol) in MeOH (10 mL) in a small Pyrex flask was irradiated in a microwave reactor (150 W, 7 min). Next, $NaBH_4$ (5 mmol) was added and the mixture was irradiated further (150 W, 30 min). After solvent removal and purification by washing the mixture with hexane, the product was recovered as light brown oil, purified by vacuum distillation. Yield 0.70 g, 70%. NMR: $\delta_H(CDCl_3)$ 3.6 (1H, s, NH), 3.8 (4H, s, $–CH_2–$), 6.9 (2H, td, $H_{5\text{-py}}$), 7.2 (2H, dd, $H_{3\text{-Py}}$), 7.5 (2H, t, $H_{4\text{-Py}}$), 8.4 (2H, dd, $H_{6\text{-Py}}$); $\delta_C(CDCl_3)$ 53.7, 124.0, 124, 138.8, 150.0, 159.7 ppm.

2.2. *Physical and spectroscopic methods*

2.2.1. Instrumental methods. NMR spectra were recorded on solutions in $CDCl_3$ or D_2O using a Bruker DPX300 spectrometer; FT-IR spectra were recorded on a Shimadzu FTIR-8400, and UV-visible spectroscopy employed a Hitachi U-2000 spectrophotometer. Microanalyses were performed by the Research School of Chemistry Microanalytical Service at the Australian National University, Canberra.

2.2.2. Potentiometric titrations. Potentiometric titrations were performed using a Metrohm 665 Dosimat burette and Metrohm 605 digital pH meter fitted with a Metrohm combined glass electrode. Measurements were fully automatic under the control of a PC using Matlab 6.5.1 software. Experiments were carried out at 25°C in

aqueous solution at constant ionic strength (0.1 mol L^{-1} $NaClO_4$) under nitrogen. Sodium hydroxide solution was prepared from NaOH pellets in freshly boiled water and stored under nitrogen. The solution was standardized by titration with 0.01 mol L^{-1} potassium hydrogen phthalate. Free ligand and metal complex data were analyzed and fitted simultaneously using a program (Globpot, written in Matlab 6.5.1) developed in Chemistry at the University of Newcastle. For analysis, the data, a proposed model, initial concentrations, and estimates of log β values are required.

2.2.2.1. *Ligand titration.* A solution of 0.1 mol L^{-1} NaOH was added to a solution containing approximately 1.5×10^{-3} mol L^{-1} ligand as well as excess acid ($HClO_4$) of between 10% and 100%. The volume of ligand solution used was between 3 and 20 mL. The increment size and total volume of NaOH solution added was adjusted to achieve reasonable steps and titration performed to a final pH of ~12.

2.2.2.2. *Complex titration.* The complex was prepared *in situ* from approximately 1.5×10^{-3} mol L^{-1} ligand solution by addition of ~0.3 to ~0.9 equivalents of M^{2+} salt. Before titration, acid was added to give an excess of approximately 20%. The solution was then titrated with 0.1 mol L^{-1} NaOH in the same way as for the free ligand.

2.2.3. X-ray crystal structure determinations. Data sets were collected for crystals of $[Ni(\mathbf{1})_2](ClO_4)_2 \cdot H_2O$ and $[Zn(\mathbf{1})_2](ClO_4)_2 \cdot H_2O$ using a Bruker SMART CCD-1000 (for Ni) and Bruker-Nonius FR591 Kappa APEX II (for Zn) diffractometer employing graphite monochromated Mo-Kα radiation from a fine-focus rotating anode, operating in the ω scan mode to 56.62° 2θ (for Ni) and with φ and ω scans to 55.26° 2θ (for Zn), each measured at 150(2) Kelvin. Cell constants were obtained from a least-squares refinement against 9245 (Ni) and 9833 (Zn) reflections. The data integration and reduction were undertaken with SAINT and XPREP [17], and subsequent computations were carried out with the X-Seed graphical user interface [18]. Intensities of standard reflections recollected at the end of the experiment did not change significantly during the data collection. An empirical absorption correction was applied to the data [19, 20]. The structure was solved by direct methods with SIR97 [21], or SHELX-97 [22], and extended and refined with SHELXL-97 [22]. The asymmetric unit contains the complex, perchlorates (some disordered) and sites modeled as water oxygen. In general, non-hydrogen sites were modeled with anisotropic displacement parameters, and a riding atom model with group displacement parameters was used for hydrogen atoms. Water oxygen atoms were modeled with an isotropic displacement parameter, and no hydrogen atoms were included in the model for water molecules. For the Ni structure, one cyclohexane moiety was modeled with disorder over two positions (75 : 25), while one of the perchlorate anions was modeled 50 : 50 over two positions; for the Zn structure, one cyclohexane was modeled with limited disorder over two positions (93 : 7). Closely overlapping non-hydrogen atom positions were constrained to have the same anisotropic displacement parameters. Selected results of the structure solution appear in table 1; residuals cited in the table are $R_1 = \sum||F_o| - |F_c||/\sum|F_o|$ for $F_o > 2\sigma(F_o)$ and $wR_2 = (\sum w(F_o^2 - F_c^2)^2/\sum(wF_c^2)^2)^{1/2}$ all reflections, where $w = 1/[\sigma^2(F_o^2) + (A)^2 + (B)P]$ and $P = (F_o^2 + 2F_c^2)/3$, with parameters $A = 0.0393$, $B = 9.8494$ for Ni and $A = 0.0798$, $B = 15.1078$ for Zn. An ORTEPII [23] depiction

Table 1. A summary of X-ray diffraction data for isostructural $[Ni(\mathbf{1})_2](ClO_4)_2 \cdot H_2O$ and $[Zn(\mathbf{1})_2](ClO_4)_2 \cdot H_2O$.

Empirical formula	$C_{24}H_{38}Cl_2N_4NiO_{11}$	$C_{24}H_{38}Cl_2N_4O_{11}Zn$
Formula weight	688.19	694.85
Habit	Purple prisms	Colorless prisms
Crystal size (mm^3)	$0.46 \times 0.41 \times 0.30$	$0.28 \times 0.15 \times 0.13$
Temperature (K)	150(2)	150(2)
Mo-Kα wavelength (Å)	0.71073	0.71073
Crystal system	Orthorhombic	Orthorhombic
Space group	*Pbca* (#61)	*Pbca* (#61)
Unit cell dimensions (Å, °)		
a	9.437(2)	9.375(4)
b	19.662(3)	19.731(8)
c	31.685(5)	32.278(12)
α	90.00	90.00
β	90.00	90.00
γ	90.00	90.00
Volume ($Å^3$), *Z*	5879.2(18), 8	5971(4), 8
Calculated density (g cm^{-3})	1.555	1.546
F(000)	9245	9833
Absorption coefficient (mm^{-1})	0.906	1.065
Theta minimum, maximum (°)	4.88, 56.40	4.84, 53.22
Absorption correction T_{min}, T_{max}	0.690, 0.773	0.7546, 0.8739
Range of *hkl*	$-12 \rightarrow 12$, $-24 \rightarrow 25$, $-42 \rightarrow 41$	$-12 \rightarrow 12$, $-23 \rightarrow 25$, $-36 \rightarrow 42$
Reflections measured	55,561	27,308
Independent reflections (R_{merge})	7240 (0.0314)	6890 (0.0275)
Observed reflections ($I > 2\sigma(I)$)	5373	5751
Parameters, restraints	448	398
R_1	0.0399	0.0521
$wR_2(F^2$; all data)	0.1145	0.1551
Goodness-of-fit on F^2	1.095	1.031
$\Delta\rho_{max}$ and $\Delta\rho_{min}$ ($eÅ^{-3}$)	−0.519 and 0.970	−0.919 and 1.949

of the Ni molecular cation with 20% displacement ellipsoids is provided in figure 2; the isostructural Zn complex is not shown.

3. Results and discussion

3.1. *The N,N′,O-ligand (1)*

The amino alcohol synthesis involved refluxing an excess of cyclohexene oxide with a stirred solution of the amine in ethanol [8]. The product, **1**, was synthesized in both good purity and high yield using this traditional method. Subsequent recrystallization from ethyl acetate gave an analytically and spectroscopically pure sample, which was then employed in potentiometric titration experiments. The presence of only one structural isomer is consistent with extensive literature reports that stereospecific ring opening to the *trans* isomer occurs in this class of reactions [8].

The protonation and stability constants of **1** were determined by potentiometric titration. Stability constants are obtained as log β values, with successive log *K* defined as components of the log β values. For protonation, the validity of data was confirmed by the fit of the simple model for just two protonated species associated with the two

distinctly different nitrogen centers. The pK_a values determined were for LH (8.13 ± 0.04) and LH_2 (2.82 ± 0.09). The effect of an attached bulky cyclohexyl group on pK_a values is obvious, affecting the values of the first and second protonation constants compared with those reported for the 2-aminomethyl-pyridine parent of 8.57 and 2.14 [24]. While other *N,N′,O* close analogs have not been examined, somewhat related ligands including a pyridine and alcohol group display similar steps in pK_a values for their first two protonations, for example 4-(2-pyridylazo)resorcinol (12.3, 5.5) and salicylidine-2-aminopyridine (9.7, 6.3) [24, 25].

3.2. *Metal complexation of 1*

3.2.1. Structures of octahedral complexes. The syntheses of octahedral cobalt(III) and copper(II) complexes of $[M(\mathbf{1})_2]^{n+}$ were reported [8]. The bis(tridentate) nature of the Co(III) and Cu(II) complexes in the solid state was defined by X-ray crystallography, the former adopting *cis,cis,trans*(N_{py}) *facial* geometry and the latter forming an *all-trans facial* isomer (see figure 1), both with distorted octahedral geometry. Molecular mechanics analysis predicted the same two isomers as the most stable for those metal ions [8]. The preferred structure for the nickel(II) complex was also predicted (*cis,cis,trans*(N_{am})), but the structure was not determined. The molecular structures of the Ni(II) and the Zn(II) complexes are reported here and exhibit an alternate coordination mode for **1** with these ions.

Metal complexation with M(II) salts is readily achieved by simply mixing one equivalent of metal with two equivalents of ligand in ethanol, illustrated in section 2 for Cu(II), Ni(II), and Zn(II). Chromatography using a cation exchange resin was performed for the colored Cu(II) and Ni(II) compounds, with elution with dilute $NaClO_4$ solution yielding a single colored band which crystallized in good yield. This is indicative of a single dominant isomer, as suggested from earlier molecular mechanics analysis [8]. Although there is the possibility that two or more isomers may elute together, variation of eluting anion, including using lower eluate concentrations for slow elution, did not split the band observed, supporting a single species for Cu(II) and Ni(II) at least. Microanalysis confirmed the presence of a ratio of two ligands to one metal. The IR spectrum in each case is consistent with saturated amino alcohol complexes with bands due to the perchlorate anion (~1100, ~620 cm^{-1}) additional to ligand bands.

In the electronic spectra, broad and weak bands for the purple d^8 Ni(II) complex at 860 nm ($^3A_{2g} \rightarrow {}^3T_{2g}$) and 555 nm ($^3A_{2g} \rightarrow {}^3T_{1g}(F)$) with the third one expected to lie below 400 nm ($^3A_{2g} \rightarrow {}^3T_{1g}(P)$) but masked by charge-transfer absorbances, are consistent with octahedral high-spin Ni(II). The observed broad band in the visible region at 607 nm for the d^9 Cu(II) complex under the $^2E_g \rightarrow {}^2T_{2g}$ envelope is consistent with a *trans*-N_4O_2 donor set disposed in a tetragonally distorted octahedral environment. The d^{10} Zn(II) is spectroscopically silent in the visible region. For Jahn–Teller distorted ions like Cu(II), it is likely that the strong N-donors from two ligands bind preferentially coplanar with the metal ion, leaving the alcohol donors to interact in the two axial positions above and below the MN_4 plane; this was confirmed at least in the solid state by the X-ray crystal structure. This arrangement is not likely to be preferred for metal ions without Jahn–Teller distortion, and was confirmed to be the case for the

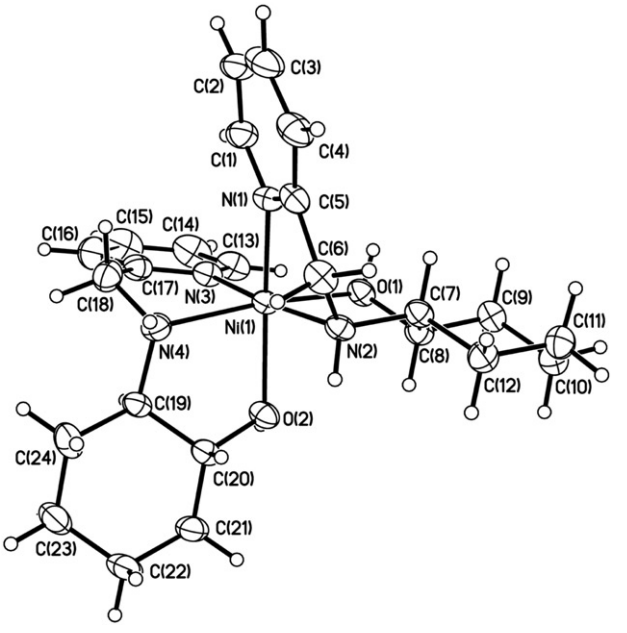

Figure 2. A view of the cation *cis,cis,cis-fac*-$[Ni(\mathbf{1})_2]^{2+}$. (The zinc complex is isostructural, and hence the cation *cis,cis,cis-fac*-$[Zn(\mathbf{1})_2]^{2+}$ is not shown separately).

Co(III) structure, where the two alcohol groups are *cis* in the solid state, from X-ray crystallography [8].

The X-ray structure of the Ni(II) complex identifies the isomer isolated as the *all-cis facial*, where each *N,N′,O*-donor ligand adopts a facial coordination mode with all three equivalent pairs of donors from each ligand in *cis* arrangements. A view of the molecule appears in figure 2, with bond lengths and angles around the metal in table 2. Earlier molecular mechanics analysis of the six possible diastereomers predicted that the *mer* and *cis,cis,trans*(*O*) isomers would be least favored, with the remaining four of similar energy, but with *cis,cis,trans*(N_{am}) predicted as favored slightly over the *cis,cis, trans*(N_{py}), *all-cis-fac* and *all-trans-fac* diastereomers [8]. It is obvious that one of this set of four has crystallized here; while not the predicted lowest energy form, the differences ($<4\,kJ\,mol^{-1}$ between any of the four) are much lower than those from this set of four to the two disfavored isomers ($\sim$10–20 $kJ\,mol^{-1}$ higher). Given the limitations of the gas-phase strain minimization optimization molecular modeling package in predicting solid state structures, whereby conclusions based on energy differences of $<10\,kJ\,mol^{-1}$ must be reached with great caution, the result is not unreasonable. Of the three structures, only in the Jahn–Teller distorted Cu(II) complex do the weaker O-donors dispose themselves in axial (*trans*) positions.

The average Ni–N(pyridine), Ni–N(amine), and Ni–O(alcohol) distances of 2.063, 2.101, and 2.105 Å, respectively, are typical of such distances found in high-spin Ni(II) compounds. With the exception of the opened out O–Ni–N(pyridine) angle (average 96.7°), the other two angles around the facially bound ligands are compressed significantly, being O–Ni–N(amine), 82.0°, and N(amine)–Ni–N(pyridine), 80.1°. This means the facial coordination is distorted and partly compressed, so most angles

Table 2. Comparisons of distances and angles around the metal for $[M(\mathbf{1})_2]^{n+}$.

Parameter	Co(III)[a]	Ni(II)[b]	Cu(II)[a]	Zn(II)[b]
Isomer isolated	*cis,cis,trans* (N_{py})-*fac*	*cis,cis,* *cis-fac*	*trans,trans,* *trans-fac*	*cis,cis,cis-fac*
M–N_{py1} (Å)	1.940(2)	2.073(3)	2.040(2)	2.145(3)
M–N_{py2} (Å)	1.938(2)	2.053(2)	2.040(2)	2.116(3)
M–N_{am1} (Å)	1.949(2)	2.094(2)	2.024(2)	2.151(3)
M–N_{am2} (Å)	1.968(2)	2.108(2)	2.024(2)	2.168(3)
M–O_a (Å)	1.9123(16)	2.0935(17)	2.3795(19)	2.182(2)
M–O_b (Å)	1.9459(16)	2.1149(18)	2.3795(19)	2.218(2)
trans X–M–X_1 (°)	174.0(1) (N_{py},N_{py})	173.62(8) (N_{py},N_{am})	163.88 (N_{py},N_{py})	171.04(10) (N_{py},N_{am})
trans X–M–X_2 (°)	177.0(1) (N_{am},O)	167.05(8) (N_{am},O)	157.64 (N_{am},N_{am})	163.01(9) (N_{am},O)
trans X–M–X_3 (°)	175.2(1) (N_{py},O)	163.56(8) (N_{py},O)	176.82 (O,O)	159.54(9) (N_{py},O)
cis O–M–O (°)	89.30(7)	89.68(7)	–	88.51(9)
cis O–M–N_{am} (°)	87.93(8), 86.40(8)	82.76(8), 86.75(8), 81.36(8)	78.82(7)	81.31(9), 84.40(10), 79.58(9)
cis O–M–N_{py} (°)	90.70(8), 93.62(8), 90.32(8), 93.86(8)	91.28(8), 97.89(8), 95.50(8)	88.42(8)	90.14(10), 100.08(10), 98.14(10)
cis N_{am}–M–N_{am} (°)	96.41(9)	105.88(8)	–	109.23(10)
cis N_{py}–M–N_{py} (°)	–	98.89(8)	–	100.35(10)
cis N_{am}–M–N_{py} (°)	84.97(9), 91.05(9), 84.18(9), 91.81(9)	79.80(8), 93.20(8), 80.38(9)	81.94(9)	78.67(10), 95.16(10), 79.72(11)

[a]Ref. [8].
[b]This study.

between the ligand pairs open a little. The presence of three different donors leads to this quite distorted octahedral geometry.

The X-ray structure of the Zn(II) complex identifies the isomer isolated as the *all-cis facial*, the same as found for Ni(II), with which it is isostructural. Bond lengths and angles around the metal are included in table 2. The average Zn–N(pyridine), Zn–N(amine) and Zn–O(alcohol) distances of 2.130, 2.159 and 2.200 Å, respectively, are typical of those found in Zn(II) compounds. These M–N distances are all from 0.06 to 0.10 Å longer than observed in the Ni(II) structure and from 0.10 to 0.20 Å longer than in the Co(III) structure. Only the Jahn–Teller elongated axis of the Cu(II) has longer metal–donor distances amongst the four structures now solved with this ligand. With the exception of the opened out O–Ni–N(pyridine) angles (average 99.1°), the other two angles around the facially bound ligands are compressed significantly, with O–Ni–N(amine), 80.5°, and N(amine)–Ni–N(pyridine), 79.2°, leaving the facial arrangement distorted and partly compressed. Angle distortions are greater than in the Ni(II) complex, tied to the longer bond lengths in the Zn(II) case.

Parameters around the metal centre for the structures of all four $[M(\mathbf{1})_2]^{n+}$ compounds appear in table 2. Coordination of **1** with three different donors leads to a distorted octahedral environment in all cases, reflected in the variable and non-ideal bond distances and angles. As the average metal–donor distance increases, greater angle

Table 3. Protonation constants and formation constants for **1** with metal(II) ions in aqueous solution. (Titrations with M : L ratios varying from 1 : 1 to 1 : 3 were examined for Cu(II) and Ni(II), but precipitation problems limited the Zn(II) study to only 1 : 1 system.)

H^+	Formed	Cu(II)		Ni(II)		Zn(II)	
pK_a	species	$\log\beta$	$\log K$	$\log\beta$	$\log K$	$\log\beta$	$\log K$
8.18 ± 0.04	ML	8.29 ± 0.16	8.29 ± 0.16	6.89 ± 0.03	6.89 ± 0.03	5.31 ± 0.03	5.31 ± 0.03
2.82 ± 0.09	ML_2	13.54 ± 0.22	5.25 ± 0.22	8.89 ± 0.21	2.00 ± 0.21	–	–
(for LH, LH_2)	$MH_{-1}L$	0.31 ± 0.19	-7.98 ± 0.19	-3.74 ± 0.02	-10.63 ± 0.02	-4.25 ± 0.06	-9.56 ± 0.06

distortion is observed; this is clearly seen (table 2) on stepping from Co(III) to Ni(II) to Zn(II), but Jahn–Teller distortion in the Cu(II) case makes it atypical. Variation in bond distances between pairs of similar donors is fairly small, except for the d^{10} Zn(II) structure.

3.2.2. Stability constants. No determinations of the stability constants of **1** with metal ions in solution have been reported previously. For labile metal(II) complexes, with compounds isolated in the solid state for Cu(II), Ni(II), and Zn(II) all being 1 : 2 M : L species, it was anticipated that such species also exist in solution. Further, it is reasonable that a 1 : 1 M : L species will exist under certain conditions. Whether higher ratio species such as 1 : 3 M : L exist depends not only on possible coordination of the potentially tridentate ligand as bidentate but also binding of three ligands, each operating in bidentate mode, to all six sites of an octahedral environment. This is unlikely at least with Cu(II), where Jahn–Teller elongation along one axis favors pseudo-square planar arrangements with strong-field N-donor ligands. The small "bite" of the *N,N′*-chelate, which forms a five-membered ring, would not permit its coordination in this mode to the one site that requires a significantly elongated bond. Polymetallic compounds are possible, where donor groups may act in bridging modes between metal ions, but there is no evidence for such species forming with **1** [8]. Consequently, it was anticipated that ML and ML_2 species would form key parts of the model for speciation in solution, perhaps with some deprotonated species also relevant. A range of different models were applied in analysis of the potentiometric titration curves, with chemical appropriateness and goodness-of-fit guiding choice of the final model.

Potentiometric titrations of **1** and Cu(II) were performed in triplicate with 1 : 1, 1 : 2, and 1 : 3 M : L ratios. In all cases, a common model could be employed, consisting of ML, ML_2, and MLH_{-1}. The involvement of only two ligands per copper is consistent with the above considerations. For titration with M : L = 1 : 1 (figure 3a), the dominant species formed is ML, which exists between pH 3.5 and 8.5, with the monodeprotonated species MLH_{-1} only becoming significant above pH 8.5. Inclusion of ML_2 in the model leads to an improvement in the fit, but it is only a minor component in this case. However, with M : L = 1 : 2 (figure 3b) or 1 : 3, the ML_2 species becomes dominant between pH 6 and 9.5, with the ML species prominent only below pH 6 and MLH_{-1} prominent only above pH 9.5. The dominance of an ML_2 species in solution where

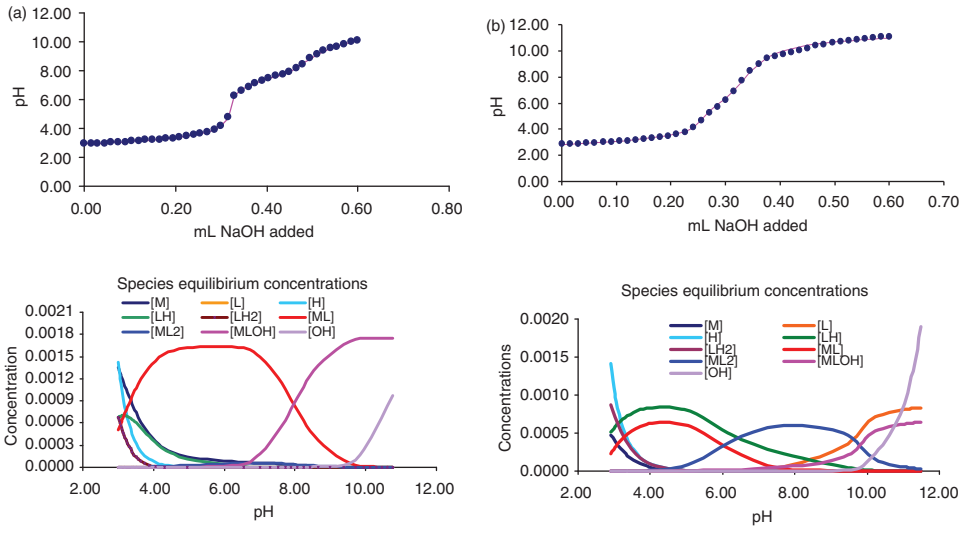

Figure 3. Titration curve (***) overlaid with calculated fit (———) (top), and species distribution curve (bottom) for the titration of **1** with Cu(II) in (a) a ~1 : 1 M : L ratio and (b) a ~1 : 2 M : L ratio [water, 0.1 mol L^{-1} $NaClO_4$, 25°C].

sufficient ligand is present matches the isolation of only an ML_2 species in the solid state.

The potentiometric titration results do not inform the details of the structure of the various species in solution, but it is almost certainly true that the ML species carries additional coordinated water molecules and may for Cu(II) be a $[Cu(\mathbf{1})(OH_2)_2]^{2+}$ complex ion with tridentate coordination of **1** and two coordinated water molecules in a classical square-based pyramidal or trigonal bipyramidal geometry commonly found for Cu(II) complexes with one tridentate ligand. The CuL_2 species in solution will certainly involve coordination of both N-donors of each ligand, most likely occupying a plane around the metal ion in the common elongated octahedral geometry, with the alcohol groups having to compete with water for the additional coordination sites. The maximum in the electronic spectrum (607 nm) supports these views, although it remains unclear if five- or six-coordination exists in solution. The deprotonated $CuLH_{-1}$ species will involve deprotonation of either a coordinated alcohol (with its pK_a reduced substantially as a result of coordination) or of a coordinated water molecule. It is not possible to distinguish between species such as $[Cu(\mathbf{1}\text{-H})(OH_2)_2]^{+}$ and $[Cu(\mathbf{1})(OH)(OH_2)]^{+}$ from this study alone, as the pK_a of ~8 can be accommodated by either proposal; the deprotonation site may even be "shared" due to the residual proton bridging between an alcohol oxygen and a water oxygen in what is an R–O···H···O–H mode. Examples of this arrangement exist in the solid state. The influence of the large cyclohexane ring on the capacity of the alcohol to bind competitively with water in solution is uncertain. However, the observation that the inert cobalt(III) complex is isolated in the solid state as a $[Co(\mathbf{1})(\mathbf{1}-H)]^{2+}$ species with a deprotonated alcohol that hydrogen bonds strongly to a protonated alcohol in another adjacent molecule is indicative of the ability of the coordinated alcohol in **1** to undergo deprotonation [8].

The model successfully employed leads to log β and log K values presented in table 3. Clearly, the ligand is a good binder of Cu(II), with log K_1 (8.3) and log K_2 (5.3) values comparable to values reported for the 2-aminomethylpyridine parent (log K_1 9.5; log K_2 5.9), and not markedly different from an array of unhindered or substituted *N*-donor chelates, such as ethane-1,2-diamine (log K_1 9.9; log K_2 6.8), 2,2-dipyridine (log K_1 10.5; log K_2 6.5), *N*-ethyl-ethane-1,2-diamine (log K_1 10.1; log K_2 7.1), and piperazine (log K_1 9.7; log K_2 5.6) [24]. The determined K_1, K_2 values and their relative closeness to those of an array of well-characterized *N,N′*-chelates are good evidence for at least *N,N′*-chelation of **1** in solution. Coordination of the alcohol may be anticipated to influence the stability constant positively leading to an additional chelate ring, even though it is not expected to be a particularly good donor in the neutral (R–OH) state. From the above comparisons of **1** with simple *N,N′*-chelates, this additional chelation is not really evident, which suggests that the alcohol group, at least in the absence of deprotonation, may not be bound strongly if at all in solution (although steric crowding may also play a role by inducing slightly weaker coordination). For Jahn–Teller distorted Cu(II), a species with unbound alcohol groups is a highly likely outcome, but it may even hold true for those metal ions that are not distorted in this way. Coordination in the solid state does not necessarily indicate the behavior in solution for labile complexes.

Potentiometric titrations of **1** and Ni(II) were performed in triplicate with each of 1 : 1, 1 : 2, and 1 : 3 M : L ratios. Models consisting of ML and MLH_{-1} or else ML, ML_2, and MLH_{-1} were best of a range examined. The involvement of no more than two ligands per nickel in modeling is consistent with outcomes in the solid state discussed earlier. For titration with M : L = 1 : 1, the simple ML and MLH_{-1}, model was sufficient, as addition of ML_2 did not improve the goodness-of-fit in this case. For higher concentrations of ligand, inclusion of an ML_2 species gave a better fit. This model is consistent with that employed for Cu(II) above. The ML species (M = Ni) is dominant between pH 4.5 and 10, with MLH_{-1} only significant above pH 10. The ML_2 species has a low stability constant and is of limited significance in the pH range 7.5–10.5. The pink-purple solution color during titration are consistent with high-spin octahedral Ni(II) and with such species being isolated in the solid state. Coordinated alcohol and water are both likely for ML, so uncertainty about the site of deprotonation in the MLH_{-1} species applies, as discussed above for the Cu(II) system.

Potentiometric titrations of **1** and zinc(II) were performed with an ~1 : 1, M : L ratio; higher ratios were impaired by precipitation problems. The model employed was simply ML and MLH_{-1}, as addition of ML_2 did not improve the goodness-of-fit significantly in this case. For the 1 : 1 M : L titration, the ML species begins to form only above pH 5 and is dominant between pH 6 and 9, with MLH_{-1} dominant above pH 9.5. The relatively low stability of the Zn(II) complex (table 3) is consistent with expectations for this d^{10} system, where no ligand field stabilization can operate.

It is notable that the order of stabilities for log K_{ML} for the three metals examined is Zn (5.3) < Ni (6.9) < Cu (8.3), which is in step with the Irving–Williams series expectations [26]. This compares with a similar trend for log K_{ML} of 2-aminomethylpyridine itself of Zn (5.2) < Ni (7.1) < Cu (9.5) [27]. While other *N,N′,O*-donor ligands tend to follow the Irving–Williams series with values comparable to those reported here, it is notable that this is not always the case; for example, the different trend Ni (4.9) < Zn (5.8) < Cu (7.3) has been reported for salicylidine-2-amino-pyridine [24]. Matching of the ligand to the metal, for example where a particular M–L distance favored by a particular metal ion lowers strain energy, can override ligand field

stabilization contributions. Where seen, a higher value for Ni(II) compared with Cu(II) may also reflect a weak high spin–low spin equilibrium operating in the former system that would affect observed stability constants in that case alone. Values for Ni(II) and Zn(II) are, like those of Cu(II), consistent with at least *N,N′*-chelation occurring. Overall, the titrations provide support for species existing in the solution with coordination modes comparable to those in the solid state.

3.3. *Complexation of 2 and comparison with 1*

Unlike **1**, the tridentate *N,N′,N*-chelate (**2**) is well-known and as a result is well-characterized [1–12], with an established coordination chemistry. Protonation and stability constants were reported at an early stage in its development as a ligand [11, 12], but may lack the precision available with modern experimental facilities and computational packages. For example, although deviation from the fit to the titration data at high pH was identified in an early study of Cu(II) complexation, fitting of a deprotonated species was not achieved [11]. As a result, it seemed appropriate to briefly revisit this ligand, which carries the same pyridine–CH_2–NH– entity as **1**, except the arm terminating in an alcohol group is replaced in **2** by a –CH_2–pyridine arm identical to the one on the other side of the secondary amine. A sample was prepared in this case by a new one-pot microwave-assisted synthesis; this has the main advantages of a much shorter reaction time, easy work up, and economic use of solvent.

The protonation and stability constants of **2** were determined by potentiometric titration techniques. The numerical results are included in table 4 and compared with values reported in some early work [11, 12]. The second and third protonations are not well-defined, as they occur close together in the high acid range. These are assigned to the two pyridine protonation steps; the primary amine has a distinctly different pK_a to those of the aromatic nitrogens (table 4). The values of the protonation constants (6.8, 2.2) are comparable with those found for similar compounds, including **1** (pK_a values of 8.1 and 2.8) and 2-aminomethylpyridine (8.5 and 2.1). Values for two closely related dipyridineamine compounds bis(3-pyridinemethyl)amine (7.1, 3.9 and 2.9) [28] and *N,N′*-bis(2-picolyl)ethane-1,2-diamine (8.2, 5.4 (amines) and 2.0 (first pyridine)) [29] are also similar to those for **2**, as anticipated.

Surprisingly, determinations of the stability constants of **2** with metal ions in solution have been limited previously. Complexes in the solid state usually show **2** bound as a tridentate ligand [30], leading to no more than 1 : 2, M : L pseudo-octahedral species with first-row transition metal complexes. It can be anticipated with reasonable certainty that a mononuclear 1 : 2 species also exist in solution, although it is reasonable that 1 : 1M : L species will exist under certain conditions. In the solid state, **2** often forms five-coordinate Cu(**2**)X_2 complexes such as the structurally defined [Cu(**2**)$(NO_3)_2$] [31].

Table 4. Protonation constants for **2** and formation constants with copper(II) determined in aqueous solution.

Species	pK_a	Literature [11, 12]	Species	log β	log K
LH	6.76 ± 0.07	7.27; 7.30	CuL	7.43 ± 0.02	7.43 ± 0.02
LH_2	2.22 ± 0.07	2.41; 2.61	CuL_2	11.90 ± 0.03	4.47 ± 0.03
LH_3	1.53 ± 0.13	1.75; 1.12	$CuH_{-1}L$	-0.70 ± 0.02	-8.13 ± 0.02

Potentiometric titrations of **2** and Cu(II), performed with 1 : 1, 1 : 2, and 1 : 3 M : L ratios, fitted in all cases a common model consisting of ML, ML_2, and MLH_{-1}; log β and log K values obtained are included in table 4. The involvement of no more than two ligands per copper is consistent with the above considerations. For titration with M : L = 1 : 1, ML is more dominant, although inclusion of ML_2 in the model leads to a clear improvement in the fit. However, with M : L = 1 : 2 or 1 : 3, the ML_2 species is dominant between pH 5.5 and 9.5, with the ML species prominent only below pH 5.5 and MLH_{-1} prominent only above pH 9.5. The formation of an ML_2 species in solution replicates behavior found with the *N,N′,O* ligand (**1**).

Although the potentiometric titration results cannot provide the structure of species formed in solution, conventional Cu(II) coordination chemistry suggests the intermediate ML species may be $[Cu(\mathbf{2})(OH_2)_2]^{2+}$ with tridentate coordination of **2** in the plane of the Cu(II) ion and two axially coordinated water groups in a trigonal bipyramidal geometry common for Cu(II) complexes. The presence of a $CuLH_{-1}$ species from pH ~9 is consistent with deprotonation of a coordinated water. Moreover, comparable behavior for **1** supports coordinated water deprotonation rather than deprotonation of alcohol. The CuL_2 species in solution will certainly involve chelation of one pyridine and the amine of each ligand to give at least a CuN_4 environment, consistent with the purple color of the solution. Jahn–Teller elongation of Cu(II) will make tridentate coordination using the axial positions less preferred than would be the case in complexes without such elongation. Ligand **2** forms reasonably strong complexes with Cu(II), with log K_1 (7.4) and log K_2 (4.5), although the values are most comparable to the values reported for simple bidentate chelates like 2-aminomethylpyridine (log K_1 9.5; log K_2 5.9) and ethane-1,2-diamine (log K_1 9.9; log K_2 6.8) [24]. While this is good evidence for at least *N,N′*-chelation of **2** in solution, the role of the third N-donor requires some discussion. The log K values measured for **2** are also very similar to those found for **1**, despite the difference in the third donor group. An O-donor, as for **1**, is expected to be a poorer binder than an N-donor (**2**); this suggests that either no great advantage is provided by weak axial binding of the third *N*-donor over that offered by an alcohol group, or else this group is not bound in solution. Since a pendant pyridine would likely lead to a protonated MLH species being defined at lower pH, for which there is no evidence in modeling of potentiometric data, tridentate binding with considerable strain lowering the stability is favored.

The secondary amine in **1** and **2** offers the opportunity to introduce a third arm, and a wide range of such examples exist for **2** but none appear to have been reported for **1**. Of those known for **2**, addition of a third (pyridine-CH_2–) arm shows the advantage of moving to a tripodal ligand structure [32]. This tris((pyridine-2-yl)methyl)amine forms a much stronger complex with Cu(II) ($\log K_{ML} = 17.6$) than does **2** ($\log K_{ML} = 7.4$). This suggests that addition of a third coordinating arm to **1** should significantly improve its capacity to bind metal ions, which is under exploration.

Supplementary material

Crystallographic data for the two structures have been deposited with the Cambridge Crystallographic Data Centre as CDC830806 (for $[Ni(\mathbf{1})_2](ClO_4)_2 \cdot H_2O$) and CDC830807 (for $[Zn(\mathbf{1})_2](ClO_4)_2 \cdot H_2O$). Copies can be obtained free of charge from

CCDC, 12 Union Road, Cambridge CB2 1EZ, UK (Fax: +44-1223-336033; E-mail: deposit@ccdc.cam.ac.uk).

References

[1] M. Mousseron, J. Jullien, Y. Jolchine. *Bull. Soc. Chim. France*, 757 (1952).
[2] J.A. Deyrup, C.L. Moher. *J. Org. Chem.*, **34**, 175 (1969).
[3] A. Solladie-Cavallo, M. Bencheqroun. *J. Org. Chem.*, **57**, 5831 (1992).
[4] C.E. Harris, G.B. Fisher, D. Beardsley, L. Lee, C.T. Goralski, L.W. Nicholson, B. Singaram. *J. Org. Chem.*, **59**, 7746 (1994).
[5] A.S. De Sousa, R.D. Hancock. *J. Chem. Soc., Chem. Commun.*, 415 (1995).
[6] A.S. De Sousa, R.D. Hancock, J.H. Reibenspies. *J. Chem. Soc., Dalton Trans.*, 939 (1997).
[7] A.S. De Sousa, R.D. Hancock, J.H. Reibenspies. *J. Chem. Soc., Dalton Trans.*, 2831 (1997).
[8] M.J. Robertson, G.A. Lawrance, M. Maeder, P. Turner. *Aust. J. Chem.*, **57**, 483 (2004).
[9] R. Viswanathan, M. Palaniandavar, T. Balasubramanian, P.T. Muthiah. *J. Chem. Soc., Dalton Trans.*, 2519 (1996).
[10] J.K. Romary, R.D. Zachariasen, J.D. Barger, H. Schiesser. *J. Chem. Soc. C*, 2884 (1968).
[11] (a) J.K. Romary, J.E. Bunds, J.D. Barger. *J. Chem. Eng. Data*, **12**, 224 (1967); (b) J.K. Romany, J.D. Barger, J.E. Bunds. *Inorg. Chem.*, **7**, 1142 (1968).
[12] D.W. Gruenwedel. *Inorg.Chem.*, **7**, 495 (1968).
[13] S. Bhattacharya, K. Snehalatha, S.K. George. *J. Org. Chem.*, **63**, 23 (1998).
[14] S. Bhayyacharya, K. Snehalatha, V.P. Kumar. *J. Org. Chem.*, **68**, 2741 (2003).
[15] J. Glerup, P.A. Goodson, D.J. Hodsgson, K. Michelsen, K.M. Nielsen, H. Wehe. *Inorg. Chem.*, **31**, 4611 (1992).
[16] S.I. Kirin, P. Dubon, T. Weyhermuller, E. Bill, N. Metzler-Nolte. *Inorg. Chem.*, **44**, 5405 (2005).
[17] Bruker. *SMART, SAINT and XPREP. Area Detector Control and Data Integration and Reduction Software*, Bruker Analytical X-ray Instruments Inc., Madison, WI, USA (1995).
[18] L.J. Barbour. *J. Supramol. Chem.*, **1**, 189 (2001).
[19] R.H. Blessing. *Acta Cryst.*, **A51**, 33 (1995).
[20] G.M. Sheldrick. *SADABS. Empirical Absorption Correction Program for Area Detector Data*, University of Göttingen, Germany (1996).
[21] A. Altomare, M.C. Burla, M. Camalli, G.L. Cascarano, C. Giacovazzo, A. Guagliardi, A.G.G. Moliterni, G. Polidori, R.J. Spagna. *Appl. Cryst.*, **32**, 115 (1999).
[22] G.M. Sheldrick. *SHELX97 Programs for Crystal Structure Analysis*, University of Göttingen, Institüt für Anorganische Chemie der Universität, Tammanstrasse 4, D-3400 Göttingen, Germany (1998).
[23] C.K. Johnson. *ORTEPII. Report ORNL-5138*. Oak Ridge National Laboratory, Oak Ridge, TN (1976).
[24] (a) A. Martell, R. Smith, *Critical Stability Constants*, Vol. 2, Plenum Press, New York (1974); (b) D.D. Perrin, *Stability Constants of Metal Ion Complexes. Part B: Organic Ligands*, IUPAC, Pergamon Press, Oxford (1979).
[25] W.J. Geary, G. Nickless, F.H. Pollard. *Anal. Chim. Acta*, **27**, 71 (1962).
[26] H.N.M. Irving, R.J.P. Williams. *J. Chem. Soc.*, 3192 (1953).
[27] R.C. Lacoste, A.E. Martell. *Inorg. Chem.*, **3**, 881 (1964).
[28] J.K. Romary, R.D. Zachariasen, J.D. Barger, H. Schiesser. *J. Chem. Soc. C*, 2884 (1960).
[29] C. Gabriel, S. Gabriel, E.H. Grant, B.S.J. Haltsted, D.M.P. Mingos. *Chem. Soc. Rev.*, **27**, 213 (1988).
[30] J.A. McCleverty, T.J. Meyer (Eds). *Comprehensive Coordination Chemistry II: From Biology to Nanotechnology*, Elsevier, Oxford (2003).
[31] K.-Y. Choi, H. Ryu, N.-D. Sung, M. Suh. *J. Chem. Crystallogr.*, **33**, 947 (2003).
[32] E.A. Ambundo, M.-V. Deydier, A.J. Grall, N. Aguera-Vega, L.T. Dressel, T.H. Cooper, M.J. Heeg, L.A. Ochrymowycz, D.B. Rorabacher. *Inorg. Chem.*, **38**, 4233 (1999).